

# Synthesis and characterization of sulphonated polyurethane ionomers based on toluene diisocyanate

Y. Samuel Ding\*, Richard A. Register, Chang-zheng Yang†, and Stuart L. Cooper‡

Department of Chemical Engineering, University of Wisconsin – Madison, Madison, WI 53706, USA

(Received 15 July 1988; accepted 26 October 1988)

A series of elastomeric sulphonated polyurethane ionomers based on toluene diisocyanate (TDI) and one of three polyols was studied. These materials contain no chain extender; all elastomeric character is due to ionic aggregation. The choice of cation has little effect on the glass transition temperature of the matrix, which decreases with polyol molecular weight. The rubbery plateau modulus was found to vary with cation and casting solvent due to differing degrees of phase separation between ionic and polyol material. The ultimate properties of ionomers based on poly(tetramethylene oxide) polyols suggest that stress crystallization occurs at high elongations, in analogy with segmented polyurethanes and ionenes. However, the strain required to develop crystallinity varied with the neutralizing cation, due to relaxation of the matrix chains by ion-hopping, as shown by stress-strain testing and infra-red dichroism data.

(Keywords: ionomer; polyurethane ionomer; infra-red dichroism; differential scanning calorimetry; dynamic mechanical analysis; stress-strain)

## INTRODUCTION

Ionomers are copolymers containing a small amount of bound ionic functionality, most frequently sulphonate or carboxylate salts. Due to the great difference in polarity between the ionic groups and the polymer backbone, the ionic groups microphase-separate from the polymer matrix, acting as reinforcing fillers, thermally reversible crosslinks, and ion transport pathways<sup>1-5</sup>. Factors such as ion content, chain architecture, compatibility between the ions and the matrix, type of cation and anion, and thermal and mechanical history can all affect an ionomer's microstructure, so a clear understanding of ionomer structure-property relationships is invaluable. Toward this goal, a study was undertaken to probe the morphology and properties of a series of polyurethane ionomers of different polyol type, ion content and neutralizing cation. These polymers, because of their regular chain architectures, can serve as well defined 'model' ionomers.

The ionomers studied were prepared from 1:1 copolymers of toluene diisocyanate (TDI) and one of several macroglycols (polyols). The base polyurethanes have no chain extender, and thus no 'hard segment' and no tendency to microphase-separate. The chemical structure of a sulphonated polyurethane ionomer based on polytetramethylene oxide polyol of number-average molecular weight 1000 (PTMO-1000) and TDI is shown in an idealized form in *Figure 1*. As the derivatization step<sup>6</sup> takes place only at the urethane linkages, by using polyols

of different molecular weight, the ion content of the ionomer was altered. The polyols used herein have low polydispersities, which yields a more regular spacing between ionic groups than in random copolymer ionomers. This regularity may enhance the degree of phase separation and increase the likelihood of developing a well ordered microstructure. Parallel investigations of a series of ionomers based on PTMO-1000 and methylene bis(*p*-phenyl isocyanate), MDI, have been reported recently<sup>8,9</sup>. The results reported here are complementary to the results reported for the MDI-PTMO ionomers, and some differences between the two sets of materials are evident.

Using urethane chemistry provides great flexibility in molecular design. Polyols with a wide range of polarity were used: hydroxy-terminated polybutadiene (PBD), poly(propylene oxide) (PPO), and PTMO. Going from the non-polar PBD to the fairly polar PTMO provides a wide range of compatibility between the ionic groups and the polymer backbone. Ca<sup>2+</sup>, Ni<sup>2+</sup>, Zn<sup>2+</sup>, Ag<sup>+</sup>, Cd<sup>2+</sup>, Cs<sup>+</sup> and Eu<sup>3+</sup> forms of the ionomers were prepared by ion exchange from the as-synthesized Na<sup>+</sup> form to investigate the effect of neutralizing cation on morphology and properties.

## EXPERIMENTAL

### Sample preparation

The general synthetic route to these polyurethane ionomers has been described previously<sup>6</sup>. TDI (80% 2,4 and 20% 2,6 isomers, Aldrich Chemical Co.) was vacuum distilled. PTMO (DuPont Teracol,  $M_n = 1000$ , 2000, 2900), PPO (Aldrich,  $M_n = 1000$ , 2000), and PBD (Japan Synthetic Rubber Co.,  $M_n = 1970$ ) were degassed under

\* Present address: Baxter Healthcare Corporation, Round Lake, IL 60073, USA

† Present address: Department of Chemistry, Nanking University, People's Republic of China

‡ To whom correspondence should be addressed

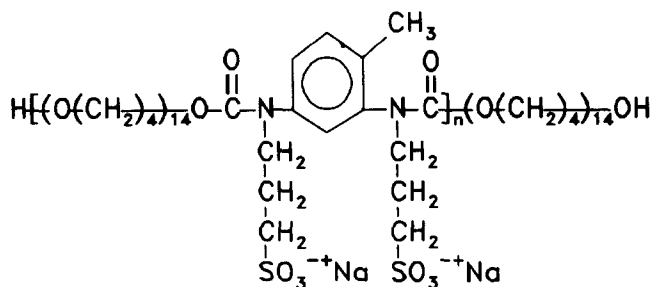


**Figure 1** Chemical structure of a sulphonated polyurethane ionomer based on PTMO-1000 and 2,4-TDI, sodium form.  $n$  is the overall degree of polymerization

vacuum at 50°C for 48 h. The polydispersity ( $M_w/M_n$ ) of the polyether polyols has been reported elsewhere to be <1.5 for PTMO<sup>7</sup> and <1.05 for PPO<sup>10</sup>. The PBD has a 1,2/1,4 content of 43/57 and a polydispersity of less than 1.2. *N,N*-dimethylformamide (DMF, Aldrich) was degassed at room temperature for 48 h. Sodium hydride (NaH, Aldrich),  $\gamma$ -propane sultone (Aldrich) and stannous octoate (catalyst T-9, M&T Chemicals) were used as received.

The polyurethane copolymers were synthesized in DMF under a nitrogen atmosphere, using 0.5 wt% T-9 catalyst. To ensure complete reaction, the mixture was kept at 100°C for 4 h. To make the ionomers, the polyurethane base polymer was first dissolved in DMF (5 wt%) and mixed with a dispersion of NaH in DMF. The reaction mixture was kept at -5°C in a salt-water-ice bath under nitrogen and vigorously stirred. After 15 min, the stoichiometric amount of  $\gamma$ -propane sultone was added and the mixture was heated at 50°C for 2 h. The reaction mixture was filtered to remove unreacted NaH and the ionomer recovered by precipitation into toluene. The ionomer was further washed and extracted with ethanol or an ethanol/heptane mixture to remove any residual  $\gamma$ -propane sultone and NaH.

This synthetic method provides the sodium salt directly. To prepare ionomers with other cations, a 5 wt% methanol solution of the sodium ionomer was converted into the acid form by passing it through a column packed with Amberlyst 15 ion-exchange resin (Aldrich). RENEUTRALIZATION was accomplished by adding stoichiometric amounts of calcium, nickel, zinc, cadmium or europium acetate, silver nitrate, or caesium hydroxide. Any unreacted metal salts were subsequently extracted from the polymer using ethanol. The compositions of the sodium forms of the samples studied are listed in Table 1. The first letter of the mnemonic code refers to the polyol type (M for PTMO, P for PPO, and B for PBD); the number is the polyol molecular weight in thousands; and the final two letters are the cation's chemical symbol.

Samples for the various experiments were prepared by spin-casting at 60°C from DMF solution (for polyether-based ionomers) or from a chloroform/methanol (5:1) mixture at 20°C (for the PBD-based ionomer). Because of poor solubility of the M1Cs material in DMF, it was cast from methanol at 20°C. To examine the effect of sample preparation on morphology and properties, some members of the M1 series were also cast from a tetrahydrofuran(THF)/water mixture (5:1 v/v) at 20°C and from methanol at 20°C. Unless otherwise noted in the discussion, the sample was cast from DMF. After

solvent evaporation in the spin caster at atmospheric pressure, the films were transferred to a vacuum oven at 60°C for a minimum of 48 h to remove the residual solvent.

#### Instrumental conditions

Survey spectra were obtained using a Nicolet 7199 Fourier transform infra-red (FTi.r.) spectrometer at a resolution of 1 cm<sup>-1</sup>. The un-ionized base polyurethane was examined as a neat film between NaCl plates, while the ionomers were examined as free-standing films. Infra-red dichroism studies were performed with the aid of a gold wire grid polarizer and a manual stretching fixture, with the sample stretch direction oriented parallel or perpendicular to the polarization direction. The sample, rather than the polarizer, was rotated, and the fixture was shifted so that the beam passed through the midpoint of the sample strip at all strain levels. The specimen was allowed to relax for 5 min after each elongation increment.

Differential scanning calorimetry (d.s.c.) thermograms were recorded using a Perkin-Elmer DSC-II interfaced to a thermal analysis data station (TADS). The TADS software provides automatic baseline correction and normalization for sample weight, which was 15 ± 2 mg. Thermograms were recorded from -150 to 220°C at 20°C min<sup>-1</sup>, then the sample was quenched at 320°C min<sup>-1</sup> to -150°C and the scan repeated. Dynamic mechanical thermal analysis (DMTA) data were obtained using a Rheometrics RSA-II at a test frequency of 1 Hz, under a dry nitrogen purge. The heating rate used was 3°C min<sup>-1</sup>, and a data point was collected every 3°C. A static strain of 0.3–0.5% was used, with a peak-to-peak oscillatory strain of 0.3%. Uniaxial stress-strain testing was performed using an Instron model TM at room temperature, in air, with a crosshead speed of 0.5 in min<sup>-1</sup> (1.3 cm min<sup>-1</sup>). Samples were stamped out with a standard ASTM D1708 die.

## RESULTS AND DISCUSSION

### Synthetic procedure

The FTi.r. spectra were used to verify the complete substitution of the urethane nitrogen, as shown in Figure 2. The top trace shows the FTi.r. spectrum for the un-ionized polyurethane based on PTMO-1000, which is a viscous liquid at room temperature. The urethane N-H stretch from 3200 to 3500 cm<sup>-1</sup> is clearly visible. This range of frequencies and the breadth of the absorption peak indicate that the urethane hydrogens are strongly hydrogen-bonded<sup>11,12</sup>. The lower trace shows the final product of the synthesis, the ionomer M1Na. The N-H stretch is no longer visible, indicating that the urethane N-H linkages have been derivatized with sulphonated alkyl groups as shown in Figure 1.

**Table 1** Elemental analysis results

Sample	Sulphur (wt%)	Ionization level (%)
M1Na	4.10	92
M2Na	2.50	96
M3Na	2.10	111
P1Na	3.32	72
P2Na	2.97	116
B2Na	2.71	103

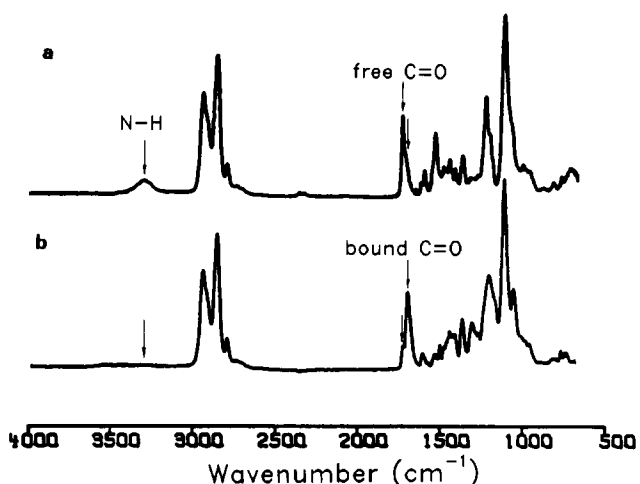


**Figure 2** FTIR spectra showing ionization of base polyurethane. (a) un-ionized PTMO-1000/TDI alternating copolymer; (b) ionized copolymer, sample M1Na

Note also that the carbonyl C=O stretch in the un-ionized material is primarily not hydrogen-bonded ( $1730\text{ cm}^{-1}$ ), indicating that most of the urethane N-H groups are hydrogen-bonding to the ether oxygens in the polyol, as expected for this single-phase material. Upon ionization, the C=O absorption decreases in frequency (to  $1705\text{ cm}^{-1}$ ), shown as 'bound C=O' in Figure 2. These frequencies are very close to those observed for 'free' and 'bound' C=O groups in polyurethanes<sup>11</sup>. Since hydrogen bonding is no longer possible after the removal of the urethane hydrogens, this may be due to the aggregation of ionic groups into microdomains, where the electronegative carbonyl oxygens are brought into contact with the ionic groups<sup>6</sup>.

To quantify the extent of reaction better, elemental analysis for sulphur was performed on several of these materials (Galbraith Laboratories). Using the known polyol molecular weights, the fractions of the urethane linkages ionized were computed, and are listed in Table 1. The ionization levels are approximately 100% for all materials studied, with the exception of P1Na, which was only 72% ionized. Some materials have a calculated ionization level  $>100\%$ . This is likely to be due to small errors in the elemental analyses or in the reported polyol molecular weights, as any unreacted  $\gamma$ -propane sultone, the only other sulphur-containing material, is removed in the synthetic procedure discussed above. In summary, the materials prepared here are essentially fully ionized, in contrast to many of the MDI-PTMO ionomers studied previously<sup>8,9</sup>, where ionization level was an important variable. Producing the M1 materials with cations other than Na allowed the effect of the neutralizing cation on morphology and properties to be examined. Wide ranges of atomic number  $Z$  (11–63), cation charge  $u$  (+1–+3), and ionic radius<sup>13</sup>  $r$  (0.69–1.67 Å\*) were used, as shown in Table 2.

### Results

Representative second-scan thermograms are shown in Figure 3, for the M1 series of materials. Each sample exhibits a single  $T_g$  at approximately  $-70^\circ\text{C}$ , corresponding to the PTMO matrix glass transition. The

neutralizing cation has little effect on the position, breadth, or magnitude of the glass transition. The  $T_g$  values for the various materials are listed in Table 3. As the polyol molecular weight is increased, the  $T_g$  drops, approaching the  $T_g$  for PTMO homopolymer<sup>14</sup>,  $-84^\circ\text{C}$ . Similar behaviour was observed previously for the PTMO-MDI polyurethane ionomers<sup>9</sup>, although not discussed there. Segments which are near the ends of the polyol chain will have their mobility sharply reduced by being tied to an ionic aggregate, thus elevating the matrix  $T_g$ . However, the fraction of such units decreases as polyol molecular weight increases, and thus the restricted mobility becomes less important and the glass transition begins to approach that for the homopolymer. Similar behaviour has been seen previously in segmented polyurethanes<sup>15</sup>.

**Table 2** Parameters of neutralizing cations

Element	Atomic number $Z$	Cation charge $u$	Ionic radius $r$ (Å)
Na	11	1	0.97
Ca	20	2	0.99
Ni	28	2	0.69
Zn	30	2	0.74
Cd	48	2	0.97
Cs	55	1	1.67
Eu	63	3	0.95

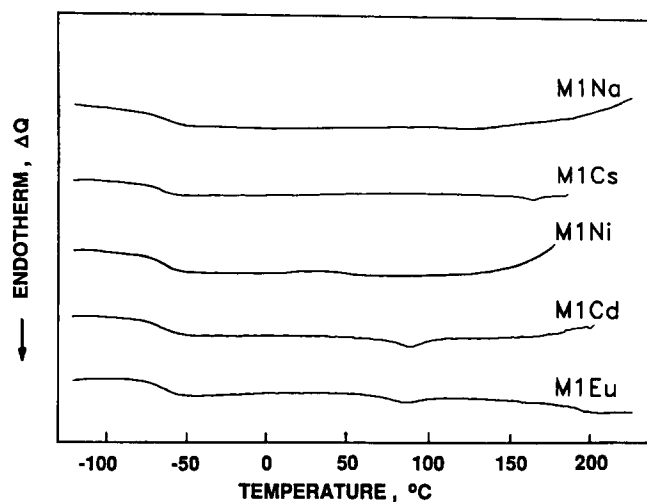


**Figure 3** Representative d.s.c. traces for the M1 series

**Table 3** Thermal analysis results

Sample/casting solvent	$T_g$ (d.s.c.) <sup>a</sup>	$T_g$ (DMTA) <sup>b</sup>
M1Na/DMF	-68.3	-73
M1Na/THF-water		-71
M1Ca/DMF	-70.1	
M1Ni/DMF	-70.1	-70
M1Zn/DMF	-68.8	-66
M1Cd/DMF	-70.8	-69
M1Eu/DMF	-67.7	-66
M1Cs/methanol	-69.0 <sup>c</sup>	
M2Na/DMF	-78.0 <sup>c</sup>	
M3Na/DMF	-81.5	
P2Na/DMF		-61
B2Na/methanol-chloroform		-60

<sup>a</sup> Midpoint of transition in second heat, unless otherwise indicated

<sup>b</sup> Maximum in  $E''$

<sup>c</sup> For first heat

\*  $1\text{ Å} = 10^{-1}\text{ nm}$

## DMTA results

Dynamic mechanical thermal analysis (DMTA) was used to explore the modulus-temperature properties of these materials as a function of casting solvent, neutralizing cation, and polyol type. The results are shown in Figures 4-6, and glass transition temperatures, taken as the maxima in the loss moduli ( $E''$ ), are listed in Table 3. Since scan rates of  $20^\circ\text{C min}^{-1}$  (d.s.c.) and 1 Hz (DMTA) are comparable in time scale<sup>16</sup>, the  $T_g$  values of the two test methods are similar. Essentially, no trend of  $T_g$  with cation is observed by either test method for the M1 materials.

In Figure 4, curves of tensile storage modulus ( $E'$ ) and loss tangent ( $\tan \delta$ ) versus temperature are shown for the M1Na material cast from two different solvents: dimethylformamide (DMF) and a tetrahydrofuran(THF)/water mixture (5:1 v/v). Both samples exhibit a wide rubbery plateau extending from approximately  $-40$  to  $90^\circ\text{C}$ , due to physical crosslinking of the material by the ionic aggregates. However,  $E'$  in the plateau region is significantly lower for the sample cast from the more polar THF/water mixture. It has been shown previously<sup>17,18</sup> that polar solvents such as water will strongly coordinate to the cations in sulphonated ionomers, decreasing their effective charge/radius ratio dramatically. This may also be expected to increase the number of ionic groups dissolved in the matrix and thereby lower the effective molecular weight between entanglements, decreasing the modulus. Several investigations<sup>19,20</sup> have shown that trace water is extremely difficult to remove from perfluorinated sulphonic acid ionomers, and heating under vacuum at  $120^\circ\text{C}$  was required to dry substantially a zinc-neutralized sulphonated polystyrene ionomer<sup>21</sup>. Although these polymers have higher glass transition temperatures than the polyurethane ionomers, and the perfluorinated ionomers are semicrystalline, which may contribute to the difficulty in drying them, it seems reasonable that the relatively mild drying conditions used here are not sufficient to remove water complexed to sulphate groups. This point will be discussed further in subsequent papers<sup>22,23</sup>.

In addition to the matrix  $T_g$  near  $-70^\circ\text{C}$ , the loss

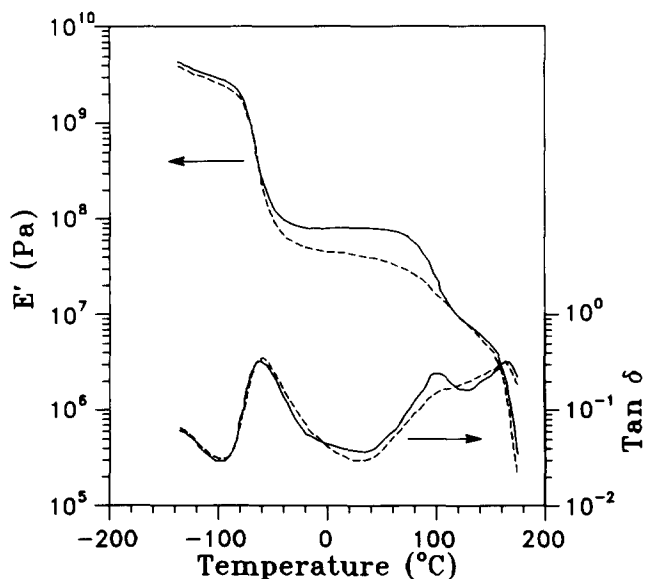


Figure 4 DMTA results,  $E'$  and  $\tan \delta$ , for the M1Na sample cast from (—), DMF, (---) THF/water

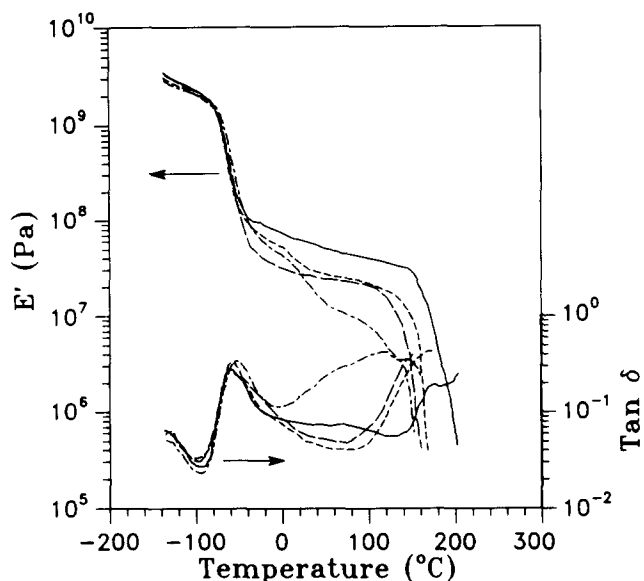


Figure 5  $E'$  and  $\tan \delta$  for (—) M1Ni, (---), M1Cd, (-·-) M1Eu, and (---) M1Zn, all cast from DMF

tangent also exhibits a peak near  $100^\circ\text{C}$  for the M1Na material, which is more pronounced when DMF is used as the casting solvent. Flow of the material, due to the decreased effectiveness of the ionic aggregates as physical crosslinks at high temperature, is observed to occur near  $160^\circ\text{C}$ , as evidenced by the steep drop-off in  $E'$ . Therefore, the transition near  $100^\circ\text{C}$  must have a different source, which may be related to dissociation or rearrangement of the ionic aggregates. A similar loss maximum has previously been observed in the sodium salts of ethylene/methacrylic acid copolymers by DMTA<sup>24</sup> and dielectric<sup>25</sup> measurements and has been attributed to a transition within the ionic domains. Because of the stronger ionic association in sulphonated than in carboxylated ionomers<sup>26</sup>, such a transition might be expected to occur at a higher temperature here. Currently, the origin of this transition remains unclear.

Figure 5 presents the DMTA data for other materials in the M1 series, all cast from DMF. Here the cation type can be seen to have a profound effect on the plateau modulus, with  $\text{Ni, Na} > \text{Eu, Cd} > \text{Zn}$ . The strains involved in DMTA are quite small ( $< 1\%$ ), so the ionic aggregates should be effective physical crosslinks for all materials. Since the polymer backbone and neutralization levels are the same for all these materials, the differences in  $E'$  may be rationalized as were the  $E'$  differences for M1Na cast from different solvents; that is, ionic groups comprising certain cations are more soluble in the PTMO matrix than others. M1Zn has the lowest plateau modulus; zinc has a relatively covalent bonding nature compared with most cations, which causes the ionic aggregates in zinc-neutralized ionomers to be relatively labile<sup>27</sup>. For example, ionomers neutralized with zinc have relatively low melt viscosities<sup>27,28</sup>. Therefore, it is reasonable to conclude that the differences in  $E'$  result from different levels of ionic groups dissolved in the matrix. It should be pointed out, however, that to make such a comparison the neutralization levels and sample preparation conditions must be identical for all samples, as was the case here. Note that the plateau moduli do not seem to correlate with the cation valency or ionic radius as listed in Table 2. Indeed, while Ni and Zn have identical valency

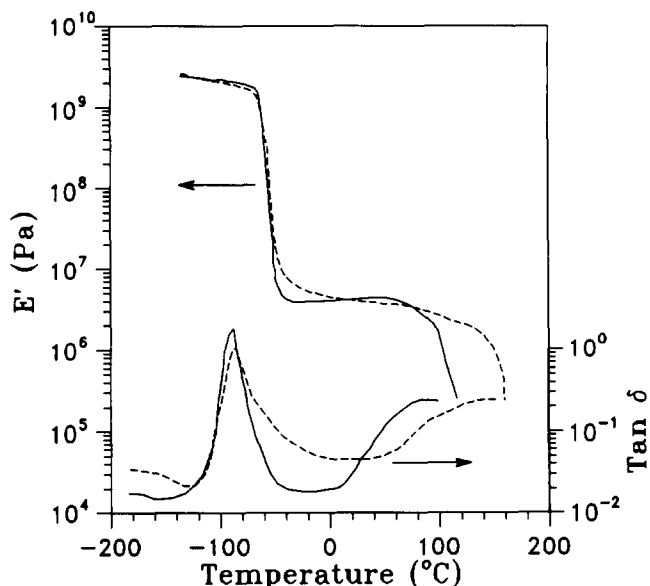


Figure 6  $E'$  and  $\tan \delta$  for (—) P2Na, cast from DMF, and (---) B2Na, cast from chloroform/methanol

and similar ionic radii, M1Ni and M1Zn have plateau moduli differing by about a factor of five. This point will be returned to in subsequent papers<sup>22,23</sup>.

Figure 6 shows the DMTA results for two ionomers based on non-polar polyols, P2Na and B2Na. Both exhibit sharp glass transitions, which is evidence for the lower degree of 'phase-mixing' (ionic groups dissolved in the matrix) expected for these non-polar polyols than the more polar PTMO. No third transition, as was observed for M1Na near 100°C, is visible in these samples. The plateau moduli for P2Na and B2Na are similar, which is understandable since the molecular weight between crosslinks is identical in the two materials. The  $E'$  values here, however, are much lower (approximately a factor of 20) than the  $E'$  value for sample M1Na, whereas the polyol molecular weight differs by only a factor of two in these materials. Therefore, polyol type as well as molecular weight appears to play a role in the small-deformation behaviour of these materials.

It is interesting to note that the P2Na material begins to flow at a substantially lower temperature (110°C) than the B2Na or M1 materials. The reason for this is unclear at present. Also, the fact that the B2Na material flows at 160°C indicates that it is not crosslinked. However, the high 1,2 content of the polyol makes it highly susceptible to crosslinking, and thus we restrict most of the following investigations to polyether-based ionomers.

Stress-strain results

DMTA probes only the small-deformation behaviour of a material, while tensile testing provides complementary large-deformation behaviour. Uniaxial stress-strain curves are shown in Figure 7 (M1 series cast from DMF), Figure 8 (M1 series cast from methanol, plus M2Na and M3Na cast from DMF), and Figure 9 (P1Na and P2Na cast from DMF). The stress ( $\sigma_b$ ) and strain ( $\epsilon_b$ ) at break for each material is listed in Table 4. As can be seen in Figures 7-9, as the polyol molecular weight increases,  $\sigma_b$  decreases, as expected based on the differing ion contents and resultant molecular weights between physical crosslinks. From Figures 7 and 8, it is clear that both the neutralizing

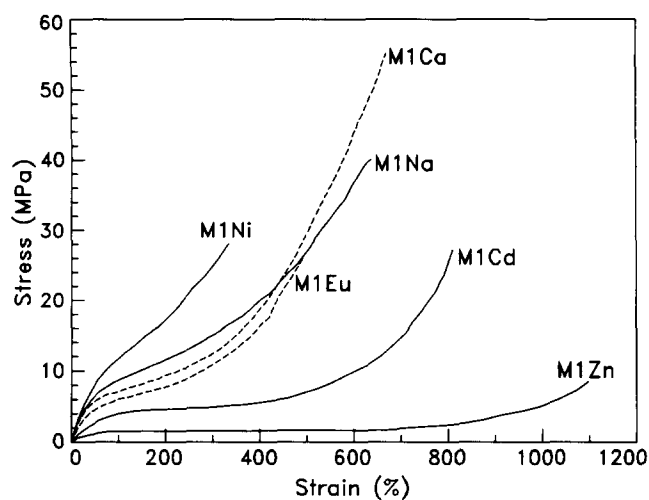


Figure 7 Uniaxial stress-strain results for members of the M1 series cast from DMF. Curves for M1Ca and M1Eu are shown as dashed lines for clarity

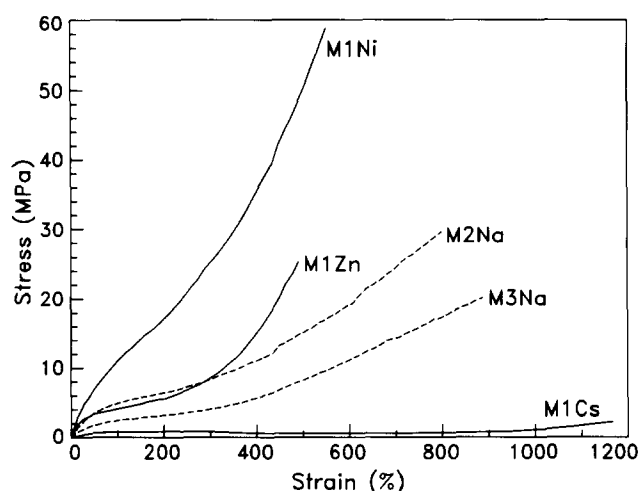


Figure 8 Uniaxial stress-strain results for members of the M1 series cast from methanol (—) and for M2Na and M3Na cast from DMF (---). Dashed lines for the latter are to emphasize the difference in polyol molecular weight

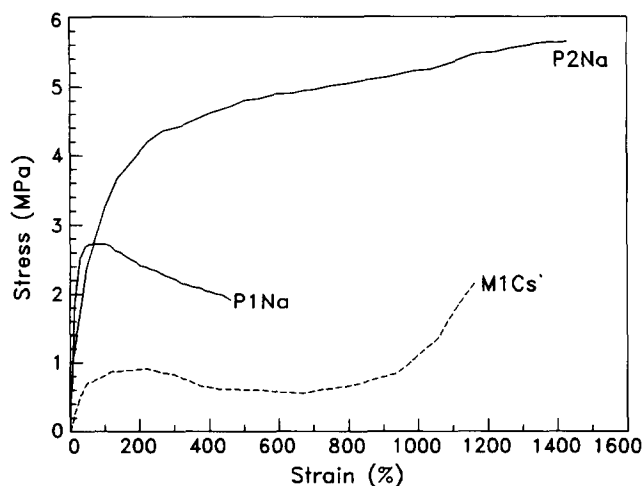


Figure 9 Uniaxial stress-strain results for P1Na and P2Na cast from DMF. The dashed curve, for M1Cs cast from methanol, is shown for comparison

Table 4 Stress-strain results<sup>a</sup>

Sample/casting solvent	$E_0$ (MPa)	$\sigma_b$ (MPa)	$\varepsilon_b$ (%)	$\alpha_c$
M1Ni/DMF	26.0	26.0	330	2.9
M1Ni/methanol	24.0	59.0	550	3.3
M1Na/DMF	25.0	40.0	640	4.0
M1Eu/DMF	19.0	26.0	490	3.3
M1Cd/DMF	17.0	27.0	810	4.6
M1Ca/DMF	23.0	55.0	670	3.5
M1Zn/DMF	8.6	8.5	1100	7.0
M1Zn/methanol	18.0	25.0	490	3.1
M1Cs/methanol	3.0	2.2	1170	7.9
M2Na/DMF	12.0	30.0	800	3.8
M3Na/DMF	7.4	20.0	890	3.9
P1Na/DMF	20.0	1.9	460	—
P2Na/DMF	9.8	5.7	1430	—

<sup>a</sup>  $E_0$  = zero-strain Young's modulus,  $\sigma_b$  = engineering stress at break,  $\varepsilon_b$  = strain at break,  $\alpha_c$  = ratio of stressed to unstressed length where Mooney-Rivlin plot exhibits a minimum

cation and the casting solvent play pivotal roles in the materials' large-deformation behaviour. For M1Ni, casting from DMF or methanol produces materials with similar moduli; however, for M1Zn, casting from methanol produces a much higher modulus than does casting from the less-polar DMF. This is surprising, since methanol should be able to coordinate to the cations at least as well, and probably better, than DMF because of specific interactions through the hydroxyl group. Indeed, it has been shown<sup>18</sup> that glycerol can effectively coordinate to the cations in zinc-neutralized sulphonated polystyrene. The explanation may lie in the difference in boiling point between the two solvents (65°C for methanol and 153°C for DMF, at atmospheric pressure). The high boiling point of DMF could make it more difficult to remove from the ionic aggregates, despite its lower polarity. The presence of DMF in the aggregates would then act as a plasticizer, causing them to be less effective as physical crosslinks. In a later paper<sup>22</sup>, it will be shown by small-angle X-ray scattering that the electron density difference between the aggregates and the polymer matrix is greater when methanol is used as the casting solvent, supporting this hypothesis. As noted previously, however, DMF was used as the casting solvent for most of these investigations.

Figure 9 shows that there is a qualitative difference in behaviour between the PTMO- and PPO-based ionomers. All PTMO-based ionomers show a strong upturn in the stress-strain curves at high elongation, which is not observed for the much weaker PPO-based ionomers. For comparison, the stress-strain curve for the weakest of the M1 series, M1Cs, is also plotted in Figure 9. This large-strain behaviour parallels that for segmented polyurethanes based on the same polyols<sup>29</sup>, where PTMO-based materials achieve much higher tensile strengths due to stress-induced crystallization of the PTMO segments. Stress-crystallization has also been observed for ionenes (polymers containing ionic groups in the backbone, rather than on side chains) based on PTMO<sup>30</sup>. It should be noted, however, that an ionomer based on MDI and PTMO-668 exhibited no PTMO crystalline spots in the wide-angle X-ray pattern<sup>9</sup>, even at 700% elongation. It was concluded in Reference 9 that no stress crystallization occurred for this low polyol molecular weight, and that the strain-hardening behaviour was due to the finite extensibility of the polyol chains. However,

it was also noted that stress crystallization might occur for higher PTMO molecular weights. Another factor inhibiting crystallization for the MDI-PTMO may have been the large fraction of un-ionized MDI units dissolved in the matrix, as the ionization level was only 25%. The qualitative difference between the M1 and P1, and M2 and P2, materials indicates that stress-crystallization is indeed operative for the materials considered here.

To quantify these tensile measurements better, the data were recast in the form:

$$[f] = \frac{\sigma}{(\alpha - 1/\alpha^2)} \quad (1)$$

where  $[f]$  is termed the reduced stress,  $\sigma$  is the engineering stress, and  $\alpha$  is the ratio of stressed to unstressed sample length. As originally noted by Mooney<sup>31</sup> and Rivlin<sup>32</sup>, tensile data for many chemically crosslinked elastomers<sup>33</sup> lie on straight lines when plotted as  $[f]$  versus  $1/\alpha$ . The Mooney-Rivlin plots for the M1 series are shown in Figure 10. For  $1/\alpha > 0.4$ , the plots are approximately linear, but at lower  $1/\alpha$  values strong positive deviations from linearity are observed due to stress-crystallization. The point  $(1/\alpha_c)$  where  $[f]$  reaches a minimum varies with cation and decreases in the order Ni > Ca > Eu > Na > Cd > Zn > Cs, as can be seen in Figure 10. Values of  $\alpha_c$  are also listed in Table 4. The stress at break,  $\sigma_b$ , will vary from specimen to specimen, as the tears which cause the sample to fail initiate at imperfections. However,  $\alpha_c$  will depend only on the material and not on flaws in the particular specimen. Thus, it is preferable to correlate structural variations with  $\alpha_c$  rather than with  $\sigma_b$ . Note that the trends in  $1/\alpha_c$  and in  $E'$  measured by DMTA, for the M1 series cast from DMF, are similar: Ni > Eu > Cd > Zn. M1Na, which has the highest plateau modulus, exhibits a  $1/\alpha_c$  value between those for M1Eu and M1Cd. However, the trends suggest a relationship between the small- and large-strain behaviour.

It is noteworthy that stress crystallization does not begin at the same extensions for different materials in the M1 series, even though the chain architectures are identical. The differences may be understood by the 'ion-hopping' mechanism<sup>34-36</sup>, which postulates that the material can flow by the redistribution of ions between aggregates, without requiring aggregate dissociation. In

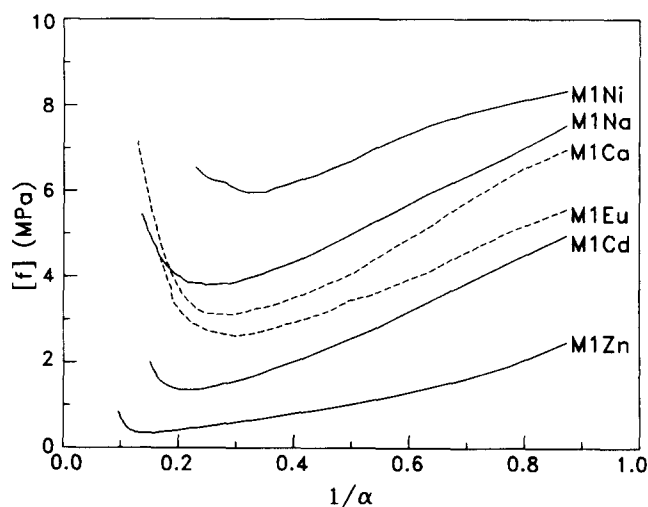


Figure 10 Mooney-Rivlin plots of the data shown in Figure 7

the present case, this suggests that in the weaker materials ion-hopping is easier than in the stronger materials, such that the onset of stress-crystallization, as shown in the  $\alpha_c$  values, is delayed by relaxation of the polyol chains. The reasons for these differences have been discussed previously for carboxy-telechelic polyisoprene ionomers<sup>37</sup> and will be discussed further in a later paper<sup>23</sup>. Again, note that the trend in  $\alpha_c$  does not appear to correlate with any of the cation parameters in Table 2.

Finally, the zero-strain Young's modulus,  $E_0$ , was obtained by linearly extrapolating the Mooney-Rivlin plots to  $\alpha=1$  (zero strain) and multiplying by 3. The trends in  $E_0$  parallel those in  $E'$ ; that is,  $E_0$  decreases smoothly with molecular weight and, for the M1 series cast from DMF,  $E_0$  decreases in the order Ni > Na > Ca > Eu > Cd > Zn. Moreover, the product of polyol molecular weight and  $E_0$  is roughly constant for M1Na, M2Na, M3Na and P1Na, P2Na, and the 'constant' is similar for both polyol types, as expected based on a simple model where the polyol chains are the elastically effective strands.

#### Infra-red dichroism

The orientation of transition moment exhibiting infra-red activity can be studied through the technique of infra-red dichroism<sup>38-40</sup>. This technique is particularly useful for multiphase polymers, since the vibrations of chemical groups which occur in only one of the phases can be studied, allowing the orientation of chain segments within that phase alone to be determined<sup>40,41</sup>. The dichroic ratio  $D$  for uniaxial deformation is defined as:

$$D = A_{\parallel}/A_{\perp} \quad (2)$$

where  $A_{\parallel}$  and  $A_{\perp}$  are the absorbances of the specimen, at a given wavenumber, with the radiation polarized parallel and perpendicular to the direction of stretch, respectively. The absorbance of a band increases as the angle between the transition moment and the direction of polarization decreases; this relationship is given by the Hermans orientation function<sup>42</sup> for the transition moment,  $f_m$ :

$$f_m = \frac{D-1}{D+2} \quad (3)$$

In general, however, the transition moment lies at an angle  $\beta$  with respect to the chain axis, while the desired quantity is  $f$ , the orientation function of the chain. The function  $f$  may be obtained from  $f_m$  by

$$f = \left( \frac{D_0+2}{D_0-1} \right) \left( \frac{D-1}{D+2} \right) \quad (4)$$

where  $D_0 = 2 \cot^2 \beta$  is the dichroic ratio which would be observed for the transition moment if the chain were perfectly oriented. Calculation of  $D_0$  requires knowledge of the angle  $\beta$ , which may often be estimated from the chemical structure of the polymer or from studies on crystalline model compounds.

In this investigation, the desired information is the orientation of the polymer matrix chains as well as chain segments within the ionic aggregates. If the degree of phase separation is high, all the urethane carbonyl groups should reside within or be attached to the ionic aggregates, while the polyol chains form the continuous matrix. Therefore, monitoring bands characteristic of the polyol and the urethane groups should allow determi-

nation of both aggregate and matrix orientation. For a polyether matrix, useful bands are the  $\text{CH}_2$  stretch at  $2940 \text{ cm}^{-1}$  and the C-O stretch at  $1125 \text{ cm}^{-1}$ , while for the aggregates the best band to use is the 'bound' urethane C=O stretch at  $1705 \text{ cm}^{-1}$ . Because of band overlap, the  $\text{CH}_2$  stretch was the best resolved for PTMO-based materials, while the C-O stretch was used for PPO-based materials. As pointed out by Wilkes<sup>38</sup>, weak or overlapped bands are poor choices, since the selection of baseline has a marked effect on the measured dichroic ratios. The values of  $\beta$  used to convert the measured  $f_m$  values to  $f$  were  $90^\circ$  for the  $\text{CH}_2$  stretch,  $35.2^\circ$  for the C-O stretch (assuming tetrahedral bond angle) and  $78^\circ$  for the C=O stretch (based on previous results for acetanilide<sup>43</sup> and poly(ethylene sebacate)<sup>44</sup>).

Figure 11 shows the orientation function  $f$  for two materials based on PTMO-1000, M1Zn and M1Na, both cast from DMF. Orientation functions for the PTMO chains are shown as circles, and for the 'bound' carbonyl groups as squares. The M1Na matrix material appears to be far more orientable than the M1Zn sample. This is consistent with the stress-strain result discussed in the previous section, where the low modulus of M1Zn reflected a greater degree of ion-hopping. If the material can relax through this mechanism, then low orientability would be expected. The behaviour of the bound C=O transition moment is enlightening as well. In the M1Zn sample, it exhibits essentially no orientation up to 520% extension. On the other hand, the C=O moment in the M1Na sample clearly exhibits orientation. This orientation becomes noticeable above roughly 250% elongation. Comparison with Figures 7 and 10, and Table 4, shows that this strain is comparable to that at which the material exhibits strain-hardening behaviour. The DMTA data indicate that the ionic aggregates in M1Na are more effective crosslinks than those in M1Zn, and thus we would expect them to exhibit less orientability. To explain the counter-intuitive results, we postulate that due to the greater ease of ion-hopping in M1Zn, the ionic groups are able to redistribute themselves to a state wherein the aggregates are relatively unstressed. Because of the

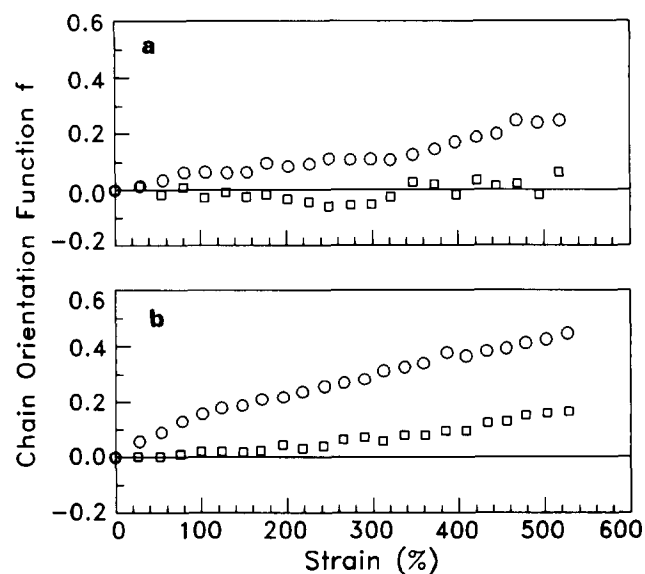
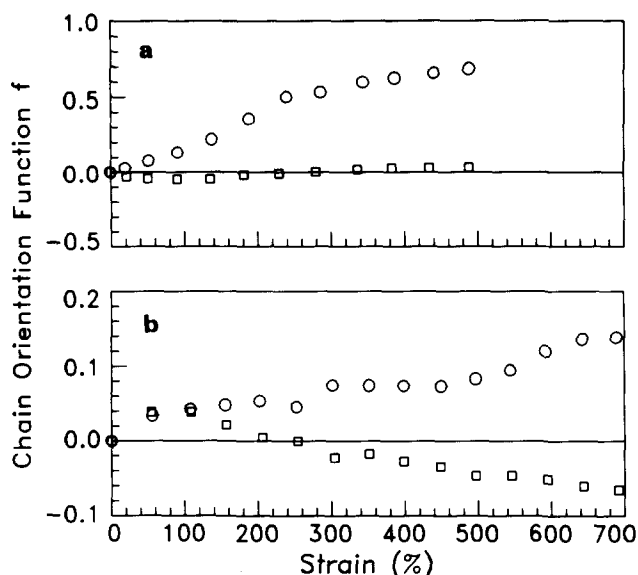


Figure 11 Infra-red dichroism results for (a) M1Zn and (b) M1Na, both cast from DMF. ○,  $\text{CH}_2$  stretch at  $2940 \text{ cm}^{-1}$ ; □, C=O stretch at  $1705 \text{ cm}^{-1}$



**Figure 12** Infra-red dichroism results for (a) M2Na and (b) P2Na, both cast from DMF.  $\circ$ ,  $\text{CH}_2$  stretch at  $2940\text{ cm}^{-1}$  (M2Na) or  $\text{C}-\text{O}$  stretch at  $1125\text{ cm}^{-1}$  (P2Na);  $\square$ ,  $\text{C}=\text{O}$  stretch at  $1705\text{ cm}^{-1}$

greater cohesiveness of the aggregates in M1Na, ion-hopping is suppressed, and the aggregates deform slightly under the strain rather than shedding ionic groups. If strain-induced crystallization is indeed occurring, then ion-hopping would be further hampered by the reduction in chain mobility due to PTMO crystallites. Note that the  $\alpha_c$  value for M1Zn is 7.0, whereas the maximum extension used in the dichroism measurements was  $\alpha = 6.2$ , so negligible stress crystallization should be expected for the M1Zn sample in the dichroism experiment.

Figure 12 shows the results for M2Na and P2Na, which differ only in polyol type; note the difference in scale between the two curves. Here, the 'bound' carbonyl groups exhibit little orientability in either case. The matrix material M2Na exhibits a much higher degree of orientability than P2Na, and considerably higher than M1Na as well. The difference between M2Na and P2Na may be easily explained by the stress-induced crystallization of PTMO, which allows for a much greater degree of orientation than in the atactic PPO. This is also expected to be the origin of the greater orientability of M2Na than M1Na, since the longer polyol chains will more easily stress crystallize. Indeed, several segmented polyurethanes<sup>15</sup> and polyurethane ionomers<sup>9</sup> based on PTMO-2000 exhibit crystallinity in the unstressed state.

## CONCLUSIONS

A series of elastomeric sulphonated polyurethane ionomers based on TDI with PTMO, PPO, and PBD polyols has been synthesized and characterized. The choice of cation was found to have little effect on the glass transition of the materials, but had a significant effect on their modulus-temperature properties and a profound effect on their stress-strain behaviour at room temperature. The rubbery plateau modulus was found to vary with cation, presumably due to differing levels of isolated ionic groups in the matrix. The addition of water to the casting solvent caused more ionic groups to be dispersed in the matrix, lowering the rubbery plateau

modulus. The zero-strain modulus decreased predictably with polyol molecular weight, but was influenced strongly by increasing the cation type and the choice of casting solvent. Otherwise equivalent materials based on PPO and PTMO have similar zero-strain Young's moduli, as determined by stress-strain testing. The high strain behaviour for ionomers based on PTMO was found to be dominated by stress-crystallization, which was absent for PPO-based materials; as a result, the PTMO materials had tensile strengths nearly an order of magnitude greater. This also resulted in far greater orientation of the matrix chains in PTMO-based materials than in PPO-based materials, as shown by infra-red dichroism.

## ACKNOWLEDGEMENTS

The authors acknowledge partial support of this research by the US Department of Energy (DE-FG02-84-ER45111) and the Division of Materials Research of the National Science Foundation (DMR 86-03839). R.A.R. wishes to thank the Fannie and John Hertz Foundation for financial support while this work was completed.

## REFERENCES

- 1 Wilson, F. C., Longworth, R. and Vaughan, D. J. *Polym. Prepr. Am. Chem. Soc. Div. Polym. Chem.* 1968, **9**, 505
- 2 Eisenberg, A. *Macromolecules* 1970, **3**, 147
- 3 Holliday, L. (Ed.) 'Ionic Polymers', Halsted-Wiley, New York, 1975
- 4 Eisenberg, A. and King, M. 'Ion-Containing Polymers', Academic Press, New York, 1977
- 5 Hsu, W. Y. and Gierke, T. D. *Macromolecules* 1982, **15**, 101
- 6 Hwang, K. K. S., Speckhard, T. A. and Cooper, S. L. *J. Macromol. Sci.-Phys.* **B23**, 153
- 7 Andrews, G. D., Vatvars, A. and Pruckmayr, G. *Macromolecules* 1982, **15**, 1580
- 8 Lee, D.-c., Register, R. A., Yang, C.-z. and Cooper, S. L. *Macromolecules* 1988, **21**, 998
- 9 Lee, D.-c., Register, R. A., Yang, C.-z. and Cooper, S. L. *Macromolecules* 1988, **21**, 1005
- 10 Dickinson, L. C., Chien, J. C. W. and MacKnight, W. J. *Polym. Prepr. Am. Chem. Soc. Div. Polym. Chem.* 1988, **29**(1), 80
- 11 Coleman, M. M., Lee, K. H., Skrovanek, D. J. and Painter, P. C. *Macromolecules* 1986, **19**, 2149
- 12 Christenson, C. P., Harthcock, M. A., Meadows, M. D., Spell, H. L., Howard, W. L., Creswick, M. W., Guerra, R. E. and Turner, R. B. *J. Polym. Sci. B Polym. Phys.* 1986, **24**, 1401
- 13 Weast, R. C. (Ed.) 'CRC Handbook of Chemistry and Physics', 59th edn, CRC Press, West Palm Beach, 1978
- 14 Lee, W. A. and Rutherford, R. A. in 'Polymer Handbook', 2nd edn, (Eds J. Brandrup and E. H. Immergut), Wiley, New York, 1975, pp. 111-157
- 15 Vallance, M. A., Castles J. L. and Cooper, S. L. *Polymer* 1984, **25**, 1734
- 16 Sperling, L. H. 'Introduction to Physical Polymer Science', Wiley, New York, 1986
- 17 Fitzgerald, J. J. and Weiss, R. A. in 'Coulombic Interactions in Macromolecular Systems', (Eds A. Eisenberg and F. E. Bailey), *ACS Symp. Ser.* 1986, **302**
- 18 Ding, Y. S., Register, R. A., Nagarajan, M. R., Pan, H. K. and Cooper, S. L. *J. Polym. Sci. B Polym. Phys.* 1988, **26**, 289
- 19 Rodmacq, B., Coey, J. M., Escoubes, M., Roche, E., Duplessix, R., Eisenberg, A. and Pinéri, M. in 'Water in Polymers', (Ed. S. P. Rowland), *ACS Symp. Ser.* 1980, **127**
- 20 Sondheimer, S. J., Bunce, N. J. and Fyfe, C. A. *J. Macromol. Sci. Rev. Macromol. Chem. Phys.* 1986, **C26**, 353
- 21 Ding, Y. S., Yarusso, D. J., Pan, H. K. and Cooper, S. L. *J. Appl. Phys.* 1984, **56**, 2396
- 22 Ding, Y. S., Register, R. A., Yang, C.-z. and Cooper, S. L. *Polymer* 1989, **30**, 1213
- 23 Ding, Y. S., Register, R. A., Yang, C.-z. and Cooper, S. L. *Polymer* 1989, **30**, 1221



*Synthesis and characterization of sulphonated polyurethane ionomers: Y. S. Ding et al.*

- 24 MacKnight, W. J., McKenna, L. W. and Read, B. E. *J. Appl. Phys.* 1967, **38**, 4208
- 25 Read, B. E., Carter, E. A., Conner, T. M. and MacKnight, W. J. *Br. Polym. J.* 1969, **1**, 123
- 26 Lundberg, R. D. and Makowski, H. S. in 'Ions in Polymers', (Ed. A. Eisenberg), *ACS Adv. Chem. Ser.* 1980, **187**
- 27 Bagrodia, S., Wilkes, G. L. and Kennedy, J. P. *Polym. Eng. Sci.* 1986, **26**, 662
- 28 Makowski, H. S. and Lundberg, R. D. *Polym. Prepr. Am. Chem. Soc. Div. Polym. Chem.* 1978, **19**(2), 304
- 29 Speckhard, T. A. and Cooper, S. L. *Rubber Chem. Technol.* 1986, **59**, 405
- 30 Feng, D., Venkateshwaran, L. N., Wilkes, G. L., Lee, B. and McGrath, J. E. *Polym. Prepr. Am. Chem. Soc. Div. Polym. Chem.* 1988, **29**(1), 134
- 31 Mooney, M. J. *J. Appl. Phys.* 1940, **11**, 582
- 32 Rivlin, R. S. *Phil. Trans. R. Soc. Lond.* 1948, **A241**, 379
- 33 Mark, J. E. *Rubber Chem. Technol.* 1975, **48**, 495
- 34 Ward, T. C. and Tobolsky, A. V. *J. Appl. Polym. Sci.* 1967, **11**, 2903
- 35 Sakamoto, K., MacKnight, W. J. and Porter, R. S. *J. Polym. Sci. A-2* 1970, **8**, 277
- 36 Hara, M., Eisenberg, A., Storey, R. F. and Kennedy, J. P. in 'Coulombic Interactions in Macromolecular Systems', (Eds A. Eisenberg and F. E. Bailey), *ACS Symp. Ser.* 1986, **302**
- 37 Register, R. A., Foucart, M., Jérôme, R., Ding, Y. S. and Cooper, S. L. *Macromolecules* 1988, **21**, 2652
- 38 Wilkes, G. L. *J. Macromol. Sci. Rev. Macromol. Chem.* 1974, **C10**, 149
- 39 Stein, R. S. *Rubber Chem. Technol.* 1976, **49**, 458
- 40 Uemura, Y., Stein, R. S. and MacKnight, W. J. *Macromolecules* 1971, **4**, 490
- 41 Estes, G. M., Seymour, R. W., Borchert, S. J. and Cooper, S. L. *Macromolecules* 1971, **4**, 452
- 42 Hermans, J. J., Hermans, P. H., Vermaas, D. and Weidynger, A. *Rec. Trav. Chim.* 1946, **65**, 427
- 43 Abbott, N. B. and Elliott, A. *Proc. Roy. Soc. Lond.* 1956, **A234**, 247
- 44 Bradbury, E. M., Elliott, A. and Fraser, R. D. B. *Trans. Far. Soc.* 1960, **56**, 1117